Title
How well will the Surface Water and Ocean Topography (SWOT) mission observe global reservoirs?

Journal
WATER RESOURCES RESEARCH, 52(3)

ISSN
0043-1397

Authors
Solander, Kurt C
Reager, John T
Famiglietti, James S

Publication Date
2016

DOI
10.1002/2015WR017952

Peer reviewed

AGU PUBLICATIONS

Water Resources Research

RESEARCH ARTICLE
10.1002/2015WR017952

How well will the Surface Water and Ocean Topography (SWOT) mission observe global reservoirs?

Kurt C. Solander[1], John T. Reager[2], and James S. Famiglietti[1,2,3]

[1]Department of Earth System Science, University of California, Irvine, Irvine, California, USA, [2]Jet Propulsion Laboratory, California Institute of Technology, Pasadena, California, USA, [3]Department of Civil and Environmental Engineering, University of California, Irvine, Irvine, California, USA

Key Points:
- Evaluated temporal and spatial error in global SWOT reservoir observations
- More elliptical reservoirs oriented parallel to orbit resulted in higher error
- Reservoir size to has the largest influence on errors except in extreme spatial settings

Correspondence to:
J. S. Famiglietti,
James.Famiglietti@nasa.jpl.gov

Citation:
Solander, K. C., J. T. Reager, and J. S. Famiglietti (2016), How well will the Surface Water and Ocean Topography (SWOT) mission observe global reservoirs?, *Water Resour. Res.*, *52*, 2123–2140, doi:10.1002/2015WR017952.

Received 3 AUG 2015
Accepted 10 FEB 2016
Accepted article online 13 FEB 2016
Published online 20 MAR 2016

Abstract Accurate observations of global reservoir storage are critical to understand the availability of managed water resources. By enabling estimates of surface water area and height for reservoir sizes exceeding 250 m^2 at a maximum repeat orbit of up to 21 days, the NASA Surface Water and Ocean Topography (SWOT) satellite mission (anticipated launch date 2020) is expected to greatly improve upon existing reservoir monitoring capabilities. It is thus essential that spatial and temporal measurement uncertainty for water bodies is known a priori to maximize the utility of SWOT observations as the data are acquired. In this study, we evaluate SWOT reservoir observations using a three-pronged approach that assesses temporal aliasing, errors due to specific reservoir spatial properties, and SWOT performance over actual reservoirs using a combination of in situ and simulated reservoir observations from the SWOTsim instrument simulator. Results indicate temporal errors to be less than 5% for the smallest reservoir sizes (< 10 km^2) with errors less than 0.1% for larger sizes (>100 km^2). Surface area and height errors were found to be minimal (area $<5\%$, height <15 cm) above 1 km^2 unless the reservoir exhibited a strong elliptical shape with high aspect ratio oriented parallel to orbit, was set in mountainous terrain, or swath coverage fell below 30%. Experiments from six real reservoir test cases generally support these results. By providing a comprehensive blueprint on the observability of reservoirs from SWOT, this study will be have important implications for future applications of SWOT reservoir measurements in global monitoring systems and models.

1. Introduction and Background

The widespread occurrence of reservoirs globally serves as a testament to the critical importance of reservoirs to water resources management. Over 50,000 global dams exist with a cumulative reservoir storage capacity totaling 7000–8300 km^3, or one-fifth of the total annual discharge to oceans [*Hanasaki et al.*, 2006; *Syed et al.*, 2010]. Water from reservoirs accounts for 30–40% of global irrigation and supports 12–16% of the world's food production [*World Commission on Dams*, 2000; *Lehner et al.*, 2011]. Recently, reservoirs have also received increased attention for their relevance to pressing environmental issues such as sea level rise [*Chao et al.*, 2008], climate change [*Schneider and Hook*, 2010], greenhouse gas emissions [*Baros et al.*, 2011] and evaporative water losses during drought (S. L. Castle, et al., Remote detection of water management impacts in the Colorado River Basin, submitted to *Geophysical Research Letters*, 2015). Due to the large number of significant studies involving reservoirs that have alerted people to global environmental change issues, reservoirs along with lakes have been termed the hydrologic "canaries in the coalmine" [*Williamson et al.*, 2009].

Given the importance of these water bodies to observations of water supplies, energy resources, and global environmental change, understanding total reservoir storage and how it varies through time is essential. Historically, reservoir observations were conducted in situ and largely confined to industrialized nations, which have more of the infrastructure in place to make such measurements. More recently, monitoring gauges worldwide have been in decline and most developing countries still do not have the financial resources or institutional mechanisms in place to make consistent and reliable measurements [*Alsdorf et al.*, 2007]. Even for those countries with the appropriate infrastructure and funds, the international sharing of reservoir operations information for research use is often not a national priority [*Famiglietti et al.*, 2015].

Within the past four decades, alternative methods of observing reservoirs have been developed through advancements in remote sensing, which has expanded the reservoir observation network to the global scale [*Yoon and Beighley*, 2014]. Remote sensing technology most relevant to direct observations of reservoirs includes satellite altimeters, optical sensors onboard orbital platforms such as the Moderate Resolution Imaging Spectroradiometer (MODIS) and Landsat satellites, as well as SAR imagery such as RADARSAT, JERS-1, and ERS. Collectively, these instruments have been used to observe changes in reservoir surface areas and height at various temporal and spatial frequencies depending on the specifications of the instrument being used [*Alsdorf et al*., 2007]. Combining these two measurements has allowed for remote estimates of reservoir storage change in a number of studies [*Zhang et al*., 2006; *Smith and Pavelsky*, 2009; *Gao et al*., 2012; *Yoon and Beighley*, 2014; *Crétaux et al*., 2015].

Unfortunately, the poor spatial and temporal frequency of measurements and interference from the land surface or weather prevents the application of these techniques over a wide range of spatial and temporal scales. In addition, use of one instrument over another often involves tradeoffs. For instance, the Landsat satellite offers a high spatial resolution of 30m for inundation area measurements, but at a low repeat orbit pass of over two weeks; whereas MODIS offers daily temporal coverage, but at a much more coarse spatial resolution of 250–500 m [*Gao et al*., 2012]. Both instruments have difficulty penetrating through clouds or smoke from forest fires [*Eilander et al*., 2014], which is particularly problematic in the low latitudes due to the persistence of the Inter-tropical Convergence Zone (ITCZ) and the common practice of biomass burning in these regions. Layover from topography or vegetation also interferes with signal trajectories leading to higher noise in signal returns. Moreover, the narrow swath widths of most altimeters leads to gaps in the spatial coverage and high wind speeds lead to larger errors in measurements by SAR imaging [*Alsdorf et al*., 2007]. Even if such issues did not exist, a lack of consistency in the timing of repeat pass cycles from satellites offering altimetry and surface area measurements hampers the ability to make regular or consistent reservoir storage change estimates. As a result, calculating storage from these techniques is typically only conducted for larger reservoirs (storage capacity > 1 km^3) because the spatial and temporal sampling and atmospheric interference issues are less of an issue for this size class [*Gao et al*., 2012].

Information obtained from the NASA Surface Water and Ocean Topography (SWOT) satellite mission (expected 2020 launch) is anticipated to dramatically improve upon existing satellite estimates of reservoirs. SWOT will produce higher spatial resolution observations of both water surface height and inundated area, allowing for more accurate estimates of changes in reservoir storage. The 78° orbit inclination allows for a maximum 21 day repeat orbit pass with an 11 day mean repeat orbit at low latitudes. The satellite will be equipped with a Ka-band swath radar interferometer capable of producing two wide swaths covering 50 km each on either side with a 20 km gap at nadir for the Ku-band altimeter. The aggregate 100 km swath width is expected to capture all lakes and reservoirs greater than 0.0625 km^2. Although offering global coverage, actual coverage is expected to be approximately 90% due to gaps in adjacent satellite tracks and spacing between nadir altimeter measurements [*Biancamaria et al*., 2015].

Based on the large quantity and distribution of reservoirs that will be monitored by SWOT and the short 3 year mission lifetime, it is essential to characterize associated measurement error prior to launch to facilitate effective processing and use of data during the mission. Anticipated major sources of error include those related to the instrument, satellite orbit, signal delay caused by the atmosphere, spatial or temporal sampling patterns, vegetation interference, layover from heterogeneities in the land surface, and supplemental data processing [*Durand et al*., 2008; *Biancamaria et al*., 2010]. Another issue is the effects of backscatter at low incidence angles over darker water surfaces where the land-water contrast is low, causing such surfaces to be incorrectly classified as terrain. More details about this problem including calibration of the backscatter coefficient can be found in *Fjørtoft et al*. [2014]. SWOT reservoir height measurements are projected to be accurate to within 10 cm for reservoirs above 1 km^2 and 25 cm for those above 0.0625 km^2 but below 1 km^2 [*Biancamaria et al*., 2015]. The expected error of reservoir surface area measurements is less than 15% of the total area [*Rodriguez*, 2015]. Even still, it is necessary to further refine these reservoir height and area error properties specifically for reservoirs, as this estimate applies to both lakes and reservoirs and is based on the properties of the instrument on-board SWOT rather than actual tests conducted exclusively for reservoirs.

Several studies have analyzed different aspects of expected river, reservoir, and lake observations or applications using SWOT. Some of these studies invoked the use of the SWOTsim instrument simulator, which

was developed to simulate expected SWOT measurements over the land surface based on realistic satellite error and orbit characteristics [*Rodriguez and Moller*, 2004]. For instance, data assimilation techniques in conjunction with simulated SWOT data produced from SWOTsim and a hydrodynamics model were used to evaluate the feasibility of estimating SWOT discharge and its expected accuracy characteristics in the Ohio River Basin [*Andreadis et al*., 2007; *Durand et al*., 2010; *Moller et al*., 2010]. Data assimilation methods were also used to compile virtual SWOT observations of reservoir elevation into a model to improve optimal releases for the Selingue Dam in the Niger River Basin [*Munier et al*., 2015]. *Pavelsky et al*. [2014] estimated how much SWOT will improve global discharge observations by determining the number of SWOT-observable river basins from an inventory of river widths developed from the Hydro1K data set. This number was then compared to in situ-observable river basins based on Global Runoff Data Centre (GRDC) and United States Geological Survey (USGS) gauge information. *Lee et al*. [2010] generated virtual SWOT measurements of lake storage changes for three large regions in the northern high latitudes using realistic SWOT spatiotemporal sampling of water surface heights from lake gauges and ENVISAT altimeter measurements, and inundated areas obtained from Landsat satellite imagery. Storage change errors of less than 5% were found for large lakes (>1 km^2) and less than 20% for small lakes (<0.01 km^2). Moreover, elongated shaped lakes were determined to have higher errors than those exhibiting a more circular geometry.

Although these studies serve as excellent prototypes for the expected accuracy of future SWOT observations in land surface hydrology and the lake error estimate studies likely bare many similarities to those for reservoirs, a number of key differences between reservoirs and lakes indicate a more detailed analysis of SWOT error properties for reservoirs is still warranted. For example, reservoir shapes tend to display a more dendritic topology and are thus more elongated with mean surface areas typically an order of magnitude higher than that of lakes, as lakes typically exhibit more rounded, symmetrical shapes. Because reservoirs are often created to augment water supplies, provide for flood control, or generate electricity, the variability in reservoir surface area and height is often much higher than that of lakes to accommodate abrupt changes in human water demands. Alternatively, lakes are defined as natural systems with generally lower water surface area and height variability linked to variations in precipitation, evaporation, and discharge. Moreover, the close linkage of reservoirs to people lends them the distinction of more likely to be located in regions with elevated human populations, such as in the low- to midlatitudes, whereas lakes are much more concentrated in the higher latitudes [*Cooke et al*., 2005]. Combined, these topologic, hydrologic, and spatial factors will likely lead to unique error characteristics in SWOT reservoir measurements relative to lakes, thereby providing the motivation for a more detailed assessment of SWOT observations of reservoirs.

In this study, we evaluate the ability of SWOT to observe reservoirs using both in situ reservoir storage records and virtual SWOT data generated from SWOTsim. First, aliasing due to the temporal resolution of SWOT is assessed by comparing "true" monthly reservoir storage computed from daily in situ storage observations to "SWOT-based" monthly reservoir storage estimates computed from subsampled in situ daily storage measurements at the expected range of SWOT repeat orbit cycles. Although we only use California reservoirs for this portion of the study, the use of the repeat orbits allows us to extrapolate the implications of the temporal results to all parts of the world covered by SWOT. Second, we use SWOTsim measurements of water surface height and area to evaluate how different spatial characteristics of reservoirs will impact the reservoir observation performance of SWOT. This information will be useful in determining the likely error characteristics for a reservoir based on its morphology or environmental settings prior to launch. Finally, we simulate SWOT measurements of water surface area and height for six California reservoirs covering three size classes using SWOTsim to provide a more realistic assessment of SWOT reservoir measurement accuracies and validate some of the results obtained from the first two components of the study.

2. Methods

2.1. Data Sources

In situ data were obtained from the California Data Exchange Center (CDEC, www.cdec.water.ca.gov, 18 August 2014). CDEC serves as a repository for statewide hydrology data from the United States Army Corps of Engineers (USACE), United States Bureau of Reclamation (USBR), and local county and municipal governments. Only data from 2008 to 2012 were used because it included both wet and dry years relative to historic statewide annual precipitation levels so a high proportion of the variability in climate information was

captured in these data sets [*NOAA*, 2014]. In addition, the use of more modern records increased the likelihood that continuous in situ data were available, thereby decreasing the need to address gaps in the record.

2.2. Temporal Analysis

For the temporal analysis portion of the study, we generate monthly "virtual SWOT" data from daily observations of reservoir storage to compare to monthly records of storage. Daily reservoir storage was obtained from 63 California reservoirs (Figure 1), which were selected based on the availability of continuous data during the targeted study period. Daily storage data from these reservoirs were subsampled at 3, 5, 10, and 20 day regular intervals to approximately match the expected SWOT repeat orbit passes over one cycle [*Biancamaria et al*., 2010]. The resulting submonthly storage data were then converted to monthly values by computing the mean out of the number of observations that fell over a given month. The computed "virtual SWOT" monthly data were compared to in situ monthly data calculated from continuous daily data using the mean percent error (ε) of storage (%) shown in equation (1):

$$\varepsilon = \frac{\sum_{i=1}^{n} [S_o(t) - S_s(t)]}{n * \sum_{i=1}^{n} S_o(t)} * 100 \quad (1)$$

where n is the number of monthly observations, S_o is the in situ monthly storage (m^3) and S_s is the monthly storage (m^3) computed from subsampled daily records.

It is acknowledged that the actual SWOT repeat orbit will occur at irregular intervals. For instance, a 5 day repeat orbit indicates SWOT will observe a location approximately four times over a 20 day period, but not necessarily every 5th day. Regular sampling frequencies are used here because we are not attempting to exactly replicate the sampling frequency of SWOT observations over the limited number of California reservoirs that were tested. Rather, we aim to capture the range of variability in error resulting from the array of expected global temporal sampling frequencies, thereby better mimicking the sample frequency error for global reservoirs and not just those in California.

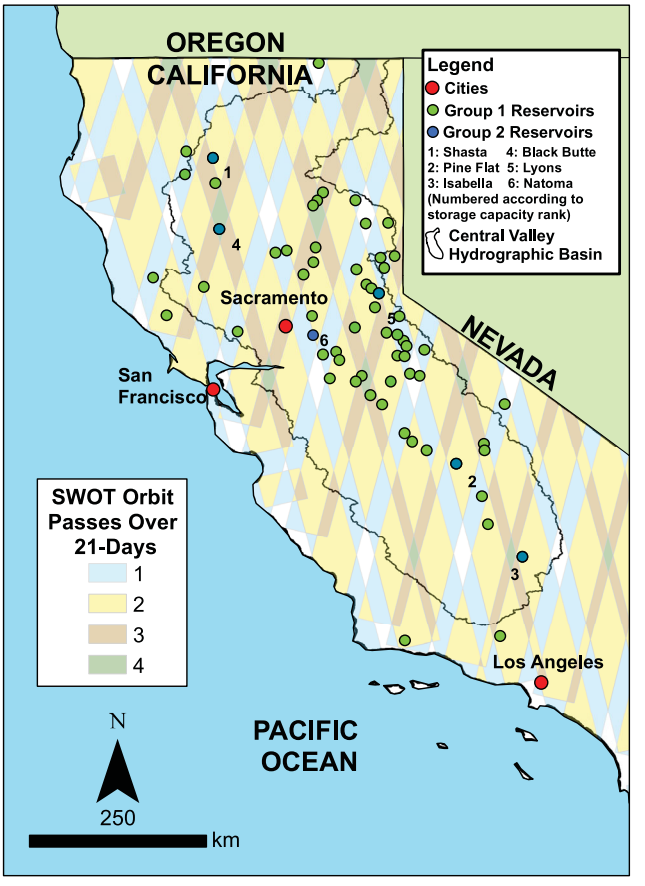

Figure 1. Location of reservoirs used in temporal analysis portion of study (Groups 1 and 2, blue and green circles) and actual reservoir test cases (Group 2, blue circles). Projected SWOT flight paths overlain for California where given swath is color-coded according to 21 day cycle repeat orbit pass (Repeat orbit pass data obtained from the Centre national d'etudes spatiales (CNES)).

2.3. Spatial Analysis: Theoretical Reservoir Experiments

The second phase of the study involved the use of SWOTsim (v2, downloaded 1 October 2014) to determine how reservoir size, shape, orientation, neighboring topography, and partial swath coverage will impact the performance of SWOT. SWOTsim involves running a series of modules to process a set of realistic SWOT orbit files, as well as digital elevation maps and water elevation files supplied by the user. Elevation and orbit information is interpolated to the sensor cross-track and along-track geometry according to the specified ground spacing input into SWOTsim. This information is then used to create the

ground-coordinate digital elevation map, which in turn, is used in conjunction with realistic radar parameters to generate the interferogram by running several additional modules [*Peral et al*., 2012]. The resulting interferogram is an image of water surface elevation swaths based on instrument errors, orbit, and spatial resolution of the satellite [*Andreadis et al*., 2007]. This provides the basis of which all simulated water surface area and elevation estimates were made using SWOTsim. More information regarding user-defined SWOTsim parameters and settings are contained in the Appendix A (Table A1).

SWOT reservoir surface area and height data were generated for theoretical reservoirs using SWOTsim, which includes a comprehensive set of expected global orbit swath paths over one 21 day SWOT cycle. The coordinates of the theoretical reservoirs were adjusted to ensure that the entire reservoir was completely within the boundaries of the orbit paths, as the theoretical experiments were designed to determine the minimum expected error in SWOT observations for different spatial characteristics.

The accuracy in reservoir surface area and height was calculated directly from SWOTsim by comparing the simulated to "truth" estimates. Errors in reservoir surface area were evaluated using the percent bias, which is shown in equation (2):

$$\theta_A = \frac{A_t - \sum_{i=1}^{k} (g_i * a_i)}{A_t} * 100 \tag{2}$$

where theta-A is the surface area bias (%), A_t is the true inundated surface area (m^2), g is the satellite ground resolution (m), a is the azimuth spacing (m) determined from SWOTsim, and k is the number of pixels associated with the observed reservoir. The product of the ground resolution and azimuth spacing is equal to the pixel area, the sum of which equals the simulated area of the given reservoir. Errors in reservoir height were calculated using the mean height bias, shown in equation (3):

$$\theta_H = \frac{\sum_{i=1}^{k} (H_t, i - H_s, i)}{n} * 100 \tag{3}$$

where theta-H is the height mean bias (%), H_t is the true and H_s is the simulated water surface height (m) given n observations. The accuracy in height observations (sigma-h) was also estimated using the root-mean-square-error (RMSE), which is shown in equation (4):

$$\sigma_H = \left[\frac{\sum_{i=1}^{k} (H_t, i - H_s, i)^2}{n} \right]^{1/2} \tag{4}$$

where H_t is the mean theoretical reservoir water surface height (m) and H_s is the simulated water surface height (m) given n observations.

Each theoretical test involved the creation of artificial reservoirs through construction of distinct water depth and digital elevation model (DEM) files, which served as the domain inputs for SWOTsim. The water depth and DEM files were developed to test only the influence of a single spatial characteristic (size, shape and orientation, topography, or partial reservoir coverage) on the performance of SWOT during each series of tests. This was achieved by holding the other spatial characteristics not actively being examined constant and using static water levels and heights to isolate the impact on observation error to only the targeted variable being tested. The number of different simulations conducted to adequately characterize the effect of a given spatial property on the error depended on the expected range of that variable likely to be observed in the real world. More details about the simulations for the different spatial tests are presented in Table 1 and in the paragraphs that follow.

The reservoir size tests proceeded by simulating SWOTsim over reservoir sizes up to 10^4 km^2, which spans the global range of reservoir surface areas (Figure 2). Only circular reservoir shapes and flat surrounding topography with static water levels were used to isolate the influence on errors to reservoir size.

The experiment for the influence of reservoir shape on SWOT observations worked similarly. For this set of simulations, only the shape of the reservoir was altered between each test. Shapes that were tested included ellipses with varying axis ratios ranging from 24:1 (more elliptical) to 1:1 (circle). This sequence was selected based on the tendency of reservoirs to form dendritic patterns comprised entirely of elongated ovals or those that more closely resemble a lake with symmetrical surface areas. For each series of aspect

Table 1. Summary Geospatial Statistics for Theoretical Reservoir Experiments

Spatial Test	No. Simulations	Area (km^2)	Aspect Ratio	Orientation Relative to Orbit (°)	Slope (m/m)	Swath Coverage[a] (%)
Size	6	10^{-1}–10^4	1:1		0	100
Shape/Orientation	18	10^0–10^2	−24:1 to 1:1	0 and 90	0	100
Topography	6	10^2	1:1		0–1.667	100
Swath Coverage	8	10^1	1:1		0	N: 2 – >50
Swath Coverage	7	10^1	1:1		0	F: 4 – >50
Swath Coverage	7	10^1	−24:1	90	0	N: 4 – >50
Swath Coverage	7	10^1	−24:1	90	0	F: 6 – >50
Swath Coverage	5	10^1	24:1	0	0	N: 1 – >50
Swath Coverage	7	10^1	24:1	0	0	F: 1 – >50

[a]N = near-range coverage, F = far-range coverage.

ratios that were tested, three different sizes were evaluated including 10^0, 10^1, and 10^2 km^2, which represent the more common reservoir sizes found globally (Figure 2). Ellipses were oriented either parallel (along-track) or perpendicular (cross-track) to the orbit pass in SWOTsim to capture the full range of reservoir shape and orientation effects on SWOT observations. Flat topography and static water levels were used.

The experiment for reservoir topography was conducted by changing the topographic slopes adjacent to the reservoir while holding all other spatial factors constant for each test. Different slopes that were used ranged from 0 to 1.7 m/m at 0.17 m/m increments. The slopes were kept uniform to a finite distance away from the reservoir to effectively form a topographic bowl on all sides of the reservoir. Only circular shapes were tested with a uniform size of 10^1 km^2 and static water levels.

The theoretical reservoir experiment involved examining the impact of partial reservoir coverage by the swath path on SWOT reservoir height observations. Note that the impact of partial reservoir coverage on inundation area measurements was not explored. This aspect was avoided because presumably when only part of the reservoir is covered by the swath, ancillary SWOT data will be used to estimate the total inundation area of the given reservoir. Partial reservoir coverages that were assessed ranged from approximately 1 to 50%, as differences in height observations did not vary by as much once the reservoir was covered by at least half of the swath. Tests were conducted separately for partial coverages in the near-range and far-range portions of the swath, as errors are not expected to be uniform throughout the swath due to larger and more variable pixel sizes in the near-range section [*Fjørtoft et al.*, 2014]. Both 1:1 and 24:1 aspect ratios oriented parallel and perpendicular to SWOT orbit were tested to capture the full range of influence from different reservoir configurations. Only flat surrounding topography with a size of 10^1 km^2 and static water levels were used for this series of experiments.

2.4. Spatial Analysis: Actual Reservoir Experiments

The final phase of this study involved the use of SWOTsim to evaluate the expected performance of SWOT for actual reservoirs. Six California reservoirs were selected based on the coverage of three size classes (<10 km^2, 10–100 km^2, and >100 km^2), as well as different spatial and climate regimes (Figure 1 and Table 2). The use of California reservoirs was ideal because like California, reservoirs at the global scale tend to be located in low- to midlatitude regions where expected SWOT orbit pass frequencies and trajectories would be similar. Only static water surface height and inundation area were investigated, as the impacts on aliasing due to the temporal resolution of SWOT were already investigated in the first part of this study. Surrounding reservoir topography was taken from the

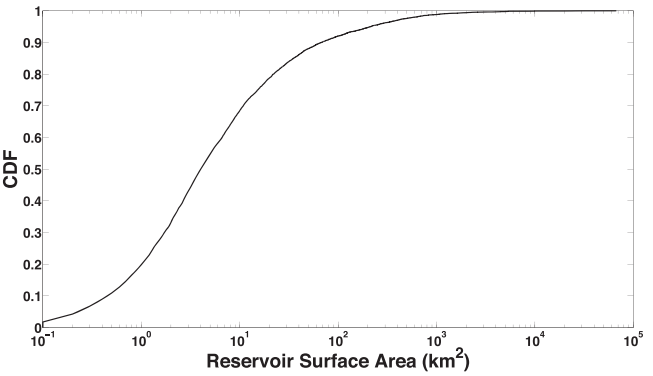

Figure 2. Global reservoir surface area Cumulative Distribution Function (CDF). Analysis incorporates data obtained from over 6000 global reservoirs [*Lehner et al.*, 2011].

Table 2. Summary Hydrology and Spatial Information for Reservoirs Used to Evaluate SWOT Performance

Reservoir Name	River	Use Code[a]	Latitude (°), Longitude (°)	Drainage Area (km^2)	Elevation (m)	Storage Capacity (km^3)	Surface Area (km^2)
Shasta	Sacramento	IMPR	40.72, −122.42	17,262	378	5.61	120.35
Pine Flat	Kings	IR	36.83, −119.33	4,002	296	1.23	24.16
Isabella	Kern	IR	35.65, −118.47	5,372	803	0.70	46.13
Black Butte	Stony	IR	39.81, −122.33	1,919	157	0.18	18.45
Natoma	American	RP	38.65, −121.19	4,916	40	0.11	2.19
Loon	Gerle	P	39.00, −120.31	21	1,944	0.09	5.86

[a]I = Irrigation; M = Municipal; P = Hydropower; R = Recreation.

NASA ASTER GDEM v2 at 30 m resolution (http://gdex.cr.usgs.gov/gdex/) due to the large increase in computation time for minimal gains in improved results at a higher spatial resolution. Reservoir inundated area bias and reservoir height mean bias were again calculated using equations (2) and (3), respectively. Multiple simulations were conducted for each reservoir where the domain was manually shifted by 0.02° longitude increments prior to each simulation until the entire width of the swath was covered to account for the differences in error properties throughout the swath. The number of simulations conducted for each of the six reservoirs is: 3, 19, 20, 15, 23, and 17 (ordered from largest to smallest by surface area).

3. Results

3.1. Temporal Analysis

The results for the portion of the study that evaluated the error due to expected SWOT observation frequencies show that smaller reservoir sizes with lower observation frequencies yield higher errors in SWOT reservoir observations. The mean monthly storage percent error (equation (1)) generally fell between 0.1 and 1% for the highest sampling frequency of one observation per every 3 days and 1–5% for the lowest sampling frequency of one observation per every 20 days. Errors between these ranges were obtained for the more moderate sampling frequencies of one measurement per every 5 and 10 days. Comparisons of monthly storage time series computed from daily (truth) and subsampled daily storage records (synthetic) at different sampling frequencies for the small ($<$10 km^2), medium (10 – 100 km^2), and large ($>$100 km^2) size classes are shown in Figure 3. The difference between the two records for any given observation did not vary by more than 1% at the highest sampling frequency and 10% at the lowest sampling frequency.

Comparable patterns were observed in the nRMSE, Nash-Sutcliffe efficiency (NSE), and 95% confidence interval results. As displayed in Figure 4, the storage nRMSE generally fell below 10^{-1} for the smaller sampling frequency and was an order of magnitude lower for the higher sampling frequency. Similarly, the NSE increased for larger reservoirs with higher sample return intervals. The NSE between true and synthetic storage records was also only observed to be consistently above 0.8 for the higher sampling frequencies of one observation per every 3, 5, and 10 days. As shown in Figure 5, the thickness of the 95% mean confidence interval in synthetic storage estimates decreased exponentially with an increase in reservoir storage capacity. The highest value of approximately 23% of maximum storage capacity was observed for the smallest reservoir at the lowest sampling frequencies. Furthermore, the 95% confidence interval width was approximately six times greater for the lowest sampling frequency relative to the highest. Mean confidence intervals approached an asymptote in reservoirs above 10 km^2 for all sampling frequencies.

3.2. Spatial Analysis: Theoretical Reservoir Experiments

Performance statistics in the theoretical reservoir size spatial experiments were also indicative of lower accuracies for smaller reservoir surface areas. As portrayed in Figure 6, the bias in reservoir surface area (equation (2)) decreased exponentially from a high of 21% to a low of less than 0.1% for the smallest 10^{-1} km^2 and largest 10^4 km^2 reservoir size classes, respectively. Correspondingly, the mean bias of reservoir height observations (equation (3)) ranged from approximately −20 cm for the smallest reservoir size to less than 1 cm for all reservoirs larger than 10^1 km^2.

In general, the theoretical reservoir shape and orientation experiments showed greater bias in water surface area and heights at higher aspect ratios (Figure 7). This scenario typically held true for each of the three size

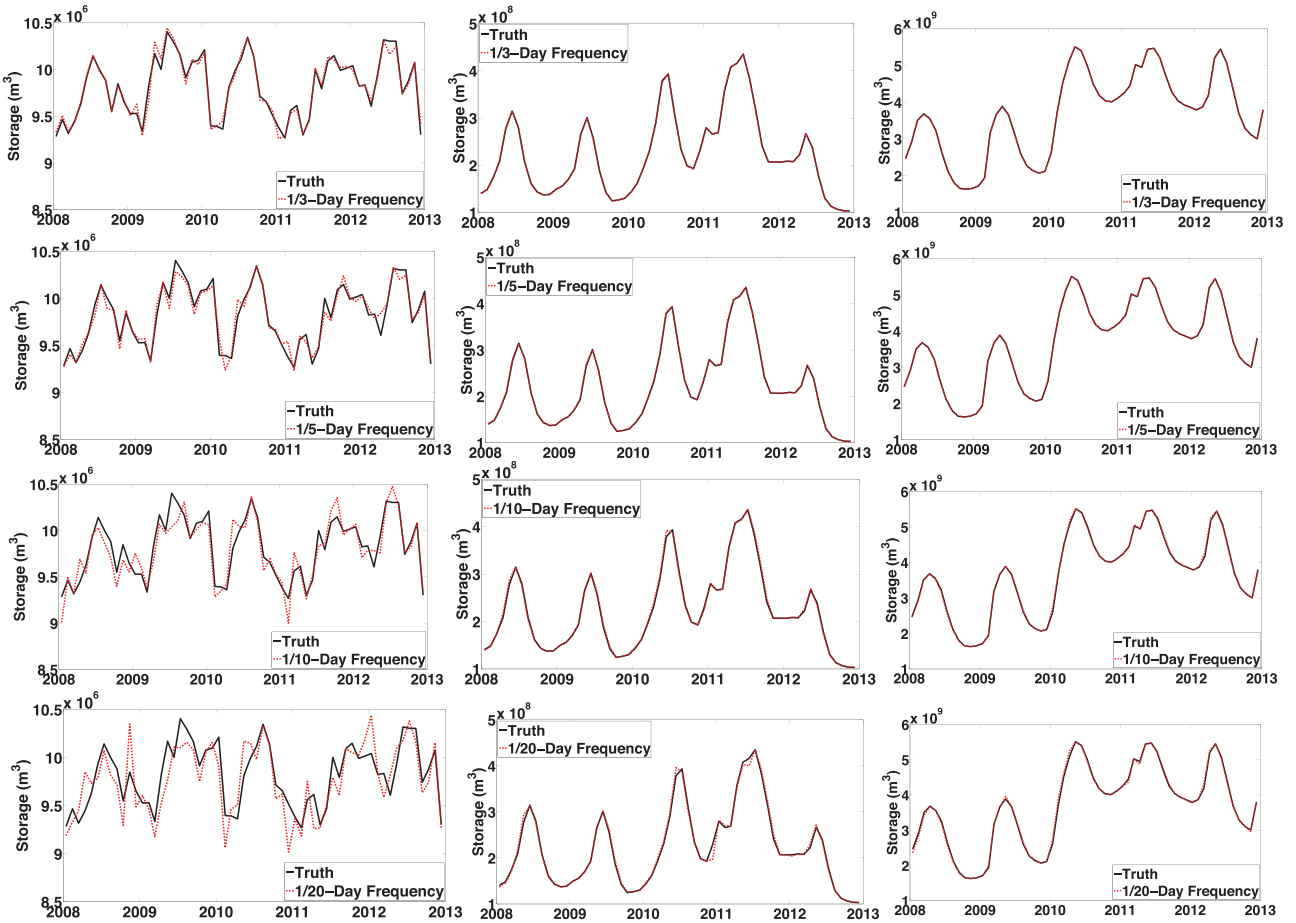

Figure 3. 2008–2012 in situ truth (black) and synthetic (red) monthly reservoir storage for the three different size classes: (left) Natoma < 10 km^2, (middle) Isabella 10–100 km^2, and (right) Shasta > 100 km^2. Analyses shown for 3 day (top), 5 day (second from top), 10 day (second from bottom), and (bottom) 20 day repeat satellite pass.

classes that were tested where the greatest bias was again observed in the smallest size class. The bias in surface area ranged between approximately 10–30% for the smallest reservoir size class of 10° km^2, but was less than 10% for all aspect ratios of the two larger size classes that were tested. Mean bias in reservoir height exhibited greater overall variability than the surface area results, but as shown in Table 3 and similar to the surface area results, the bias was higher for smaller reservoirs oriented parallel rather than perpendicular to SWOT orbit. Moreover, the percent bias in surface area increased by a factor of over two and the mean bias in height increased by a factor of more than 1.5 when the reservoir size decreased by an order of magnitude.

The test on surrounding reservoir topography revealed an increase in the magnitude of the surface area and height biases with enhancements in topographic slopes. This magnitude increase was most pronounced between slopes of approximately 0.1 m/m and 0.2 m/m for the surface area bias, while changes in the accuracy were more gradual at higher slopes (Figure 8). The mean biases in reservoir height ranged from a minimum of ± 1 cm to a maximum of -15 cm. Shifts in the accuracy of height measurements with increases in topographic slope were more variable than with the surface area results. Overall, height measurements were still less accurate at higher slopes, as the mean RMSE (equation (4)) for slopes above 0.8 m/m was 6.0 cm compared to 4.9 cm (20% decrease) below this slope threshold.

For the partial reservoir coverage tests, as expected the higher mean biases in reservoir height were associated with lower reservoir coverages for all experiments (Figure 9). The discrepancy in bias between the near and far range tests was much higher for the series of parallel to orbit trials, while this difference in magnitude was much smaller for the perpendicular to orbit and circular reservoir tests. The maximum height bias of 35 cm was observed in the near range experiments oriented parallel to orbit, while the maximum bias

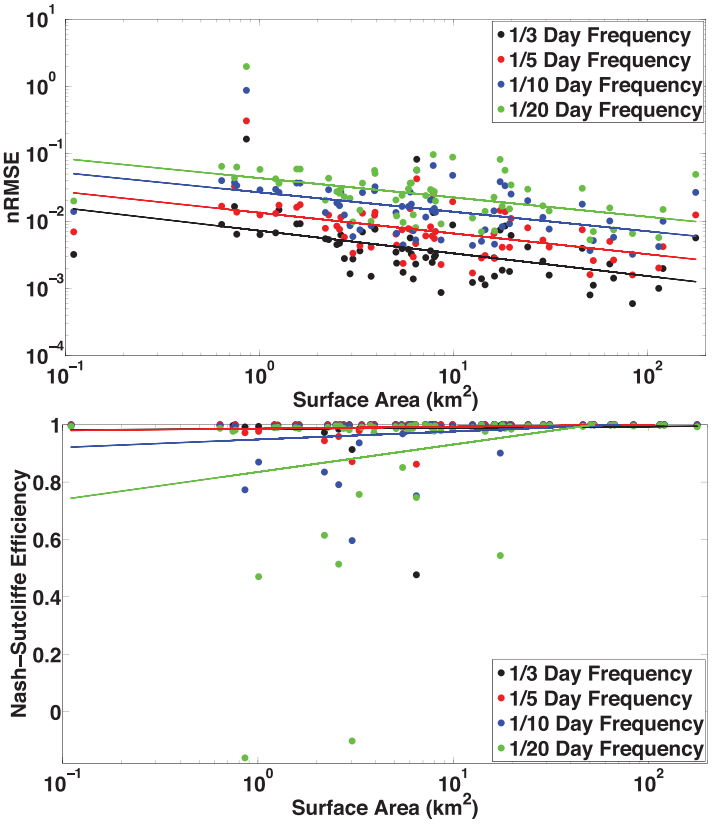

Figure 4. Normalized root-mean-squared-error (top) and Nash-Sutcliffe efficiency (btm) by reservoir storage capacity for 3 day (black), 5 day (red), 10 day (blue), and 20 day (green) sampling frequencies shown for the 63 reservoirs used in temporal analysis. Slopes of regression lines through points for different sampling frequencies are also shown. Mann-Kendall trend test with Sen's slope estimator indicate all nRMSE trends are statistically decreasing and NSE trends are statistically increasing with reservoir storage capacity ($p<0.05$).

was less than 6 cm for all other reservoir configurations and reservoir coverages that were tested. Once the swath coverage of the reservoir exceeded 30% for all experiments, the bias in reservoir height converged toward 0 cm.

3.3. Spatial Analysis: Actual Reservoir Experiments

Results from the actual reservoir simulations are presented in Figure 10. The median, 25th and 75th percentile area bias values are generally clustered close to zero for all reservoirs. The results from the smallest reservoir type represent an exception to this rule, as the median bias approached 20% with a 15–30% range for the 25th and 75th percentile values. Other 25th and 75th percentile values were close to the respective median values for the reservoir except for the fourth-largest reservoir, which had values that ranged from approximately −50 to 0%. Similar to the area bias results, low variability was observed in the mean height bias results, as the median, 25th and 75th percentile values were less than 15 cm for all but the fourth largest reservoir, which had a much higher 25th to 75th percentile range and median of approximately 25 cm. Area and height outliers outside the 25th and 75th percentiles were observed for all but the largest and fourth largest reservoirs, as well as the smallest reservoir only for the mean height bias results.

4. Discussion

4.1. Temporal Analysis

The temporal analysis portion of the study aimed to determine how well the sampling frequency of SWOT could be used to reconstruct monthly reservoir storage records. Such information will be useful for integrating into hydrologic models at similar timesteps, or for local or regional water supply monitoring systems. Moreover, this information indicates how well SWOT will be able to reproduce observations over time, as the rest of the study only evaluated error characteristics from instantaneous measurements. Based on the results, the potential for aliasing the true hydrologic signal due to the SWOT repeat orbit pass is minimal except for in the case where the smallest reservoir sizes expected to be visible by SWOT (<3 km^2) are being sampled at the lowest frequency of one observation every 20 days. Errors in individual observations for these reservoirs at this sample return interval approached 10%, which could be problematic when trying to integrate into a hydrologic model or to provide accurate information about local or regional water supplies. Based on Figure 2, approximately 40% of global reservoirs fall within this size class. Of these, only approximately one-third (13% of total) are expected to be sampled at the lowest sampling frequency where aliasing may be an issue given the global repeat orbit passes for different reservoir sizes shown in Figure 11. Nevertheless, Figure 5 indicates that above a reservoir size threshold of approximately 10 km^2 the

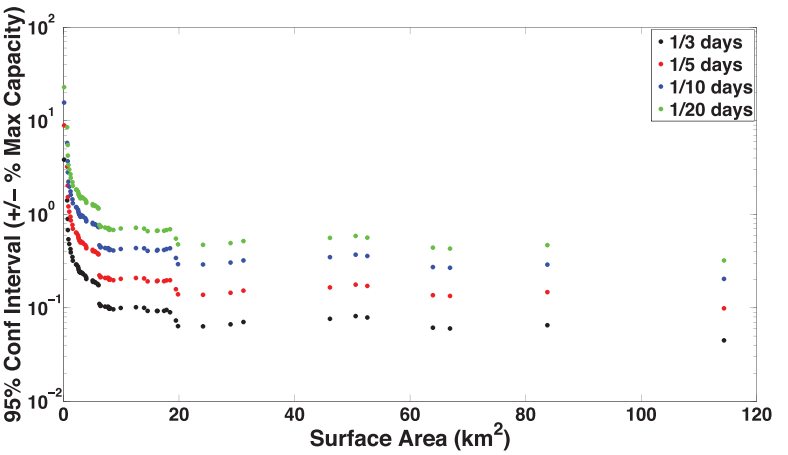

Figure 5. 95% confidence interval thicknesses for synthetic storage estimates expressed as the percent maximum capacity of the given reservoir and arranged by maximum storage capacity for 3 day (black), 5 day (red), 10 day (blue), and 20 day (green) sampling frequencies shown for the 63 reservoirs used in temporal analysis.

difference in temporal sampling error associated with reservoir size is negligible and large shifts are only related to changes in the sampling frequency. Such a finding reiterates the importance of reservoir surface area on the expected accuracy of observations.

The ability to reproduce daily or subdaily records from observations made at the range of expected SWOT sampling frequencies was not conducted as a part of this study. This information would be more beneficial for incorporating into models that use smaller timesteps or to provide useful information for reservoir functions that are more reliant on operational changes that occur over shorter timescales, such as hydroelectricity generation or flood control. Had such an analysis been performed, higher levels of aliasing would have been expected due to the large shifts in storage often associated with a single storm or abrupt snowmelt-inducing weather event that would be difficult to reproduce for all reservoir sizes at even the highest sampling frequency expected by SWOT. This was beyond the scope of this study, however, as here the interest was to evaluate the potential for aliasing at timescales that are more scalable to the temporal resolution of SWOT.

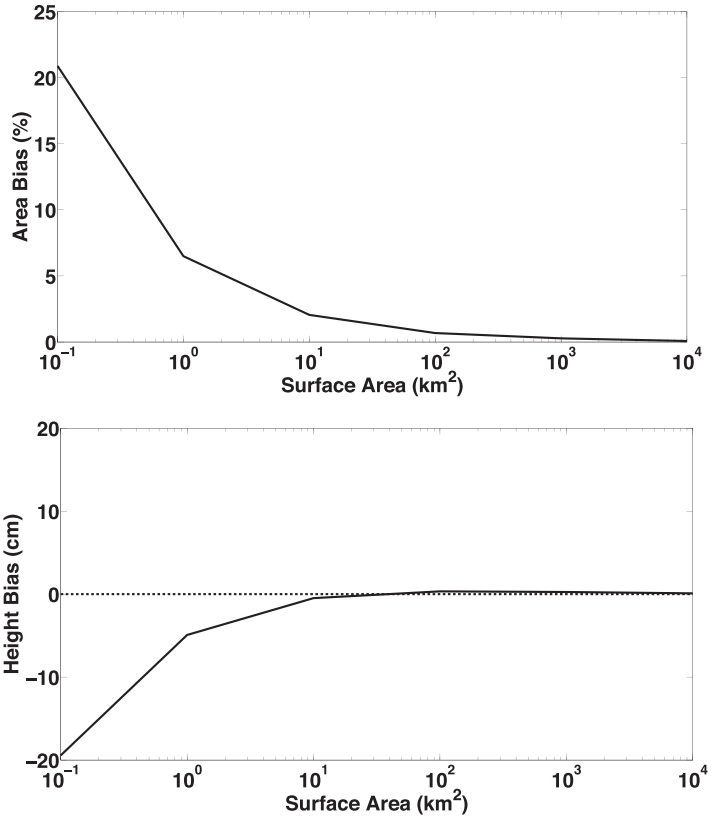

Figure 6. SWOTsim bias in reservoir surface area (top) and mean bias in water surface height (btm) for different reservoir sizes.

4.2. Spatial Analysis: Theoretical Reservoir Experiments

Many of the errors in SWOT surface water observations related to size are linked to edge effects of the given water body,

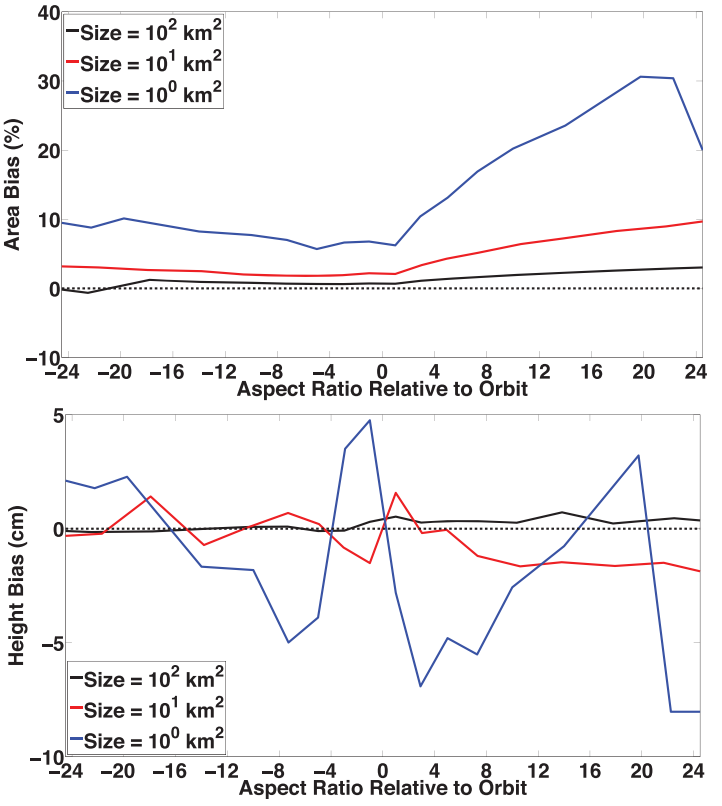

Figure 7. (top) SWOTsim bias in reservoir surface area and (bottom) mean bias in water surface height for different reservoir aspect ratios. Negative aspect ratios indicate reservoirs oriented perpendicular to orbit, while positive values denote parallel to orbit. Analyses conducted for reservoirs of size 10^2 km^2 (black), 10^1 km^2 (red), and 10^0 km^2 (blue).

meaning that higher perimeter to surface area ratios of smaller water bodies result in a lower degree of accuracy [*Lee et al.*, 2010]. Indeed, results from the theoretical experiment for reservoir size impacts on SWOT observations support this argument. Mean reservoir surface area biases of 10% were observed in reservoirs with areas that were approximately double the size threshold of 0.0625 km^2, which is listed as the minimum inundated area expected to be visible by SWOT [*Rodriguez*, 2015]. For the next highest size class of 1 km^2, the surface area bias dropped by one-half to less than 5% and continued to decrease asymptotically toward 0% for all reservoir sizes above this size. Similar trends were noted in the height bias results, as the magnitude in bias decreased exponentially from a maximum of 20 cm for the smallest 0.1 km^2 reservoir to less than 5 cm for all reservoirs above 1 km^2. Even still, given that 80% of reservoirs found worldwide are greater than 1 km^2, surface area and height error stemming from size alone should not contribute greatly to the total error for observations made by SWOT.

The SWOTsim results from the reservoir shape and orientation experiments revealed that reservoirs oriented parallel to orbit at higher degrees of ellipticity have a stronger influence on the accuracy in observations. For the perpendicular to SWOT orbit experiments, the area and height biases for all three reservoir sizes in Figure 7 more closely resemble the results for the same reservoir sizes shown in Figure 6, indicating the errors are predominantly due to the size of the reservoir. Alternatively, when the aspect ratio was oriented parallel to orbit, the area bias increased and mean height bias was more variable and reached maximum values for all three size classes at higher aspect ratios (>20:1), suggesting reservoir shape and orientation can have a much higher impact on the accuracy than size at extreme aspect ratios for the parallel to orbit case. For example, the surface area bias for the 1 km^2 reservoir size in Figure 7 is more than 350% higher than in Figure 6. In addition, as shown in Table 3, the mean height bias increased by an average of over 150%, 200%, and 400% for the 1, 10 and 100 km^2 reservoirs oriented parallel relative to those configured perpendicular to orbit. Analogous to the effects noted in the reservoir size experiments, the reduction in accuracy for large aspect ratios stems from the greater perimeter to surface area ratio and thus stronger edge effects resulting in a higher rate of landtype misidentification by the satellite.

Table 3. Reservoir Shape and Orientation Test Area and Mean Height Bias

Size (km^2)	Orientation	Mean Area Bias (%)	Mean Height Bias (cm)
10^2	Both	1.4	0.2
10^1	Both	4.3	1.0
10^0	Both	13.4	3.9
10^2	Parallel	1.8	0.4
10^2	Perpendicular	0.8	0.1
10^1	Parallel	5.9	1.3
10^1	Perpendicular	2.4	0.6
10^0	Parallel	17.7	4.7
10^0	Perpendicular	7.8	3.0

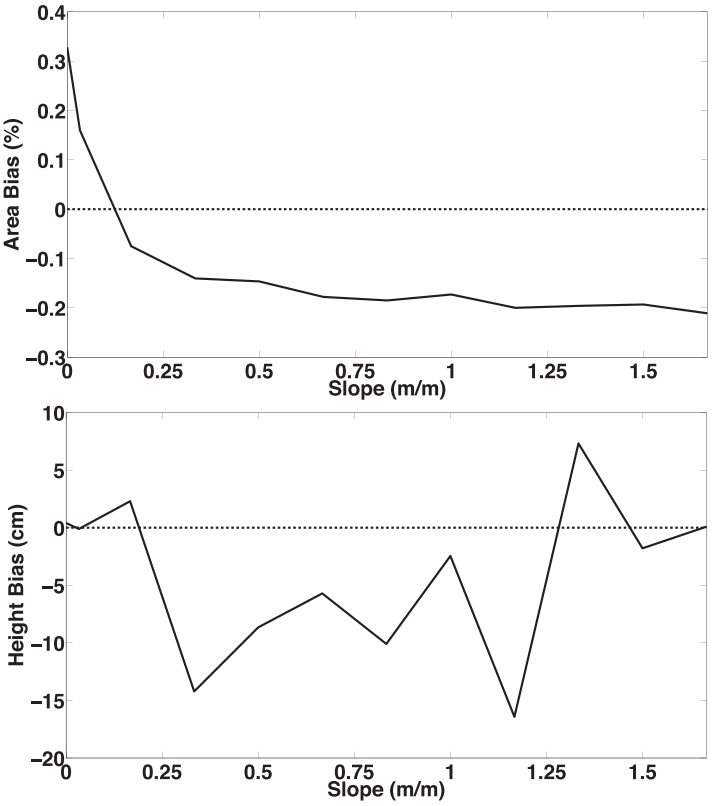

Figure 8. (top) SWOTsim bias in reservoir surface area and (bottom) mean bias in water surface height for different adjacent topographic slopes. Reservoir size held constant at 10^1 km^2 for each test.

The irregularities in the curves shown in Figure 7 can be explained by the nature of the SWOT instrumentation. For instance, the sensitivity of measurements to error is primarily a function of the mixed pixels, which are more prevalent in water bodies oriented parallel to satellite orbit because of the side-scanning arms of the interferometric Synthetic Aperture Radar on-board SWOT, which leads to an increased surface area and height bias for reservoirs with aspect ratios oriented parallel rather than perpendicular to SWOT orbit. In addition, changes in accuracy are expected when swath coverage of the reservoir switches from dominance in the far-range to the near-range portion of the swath, as projected pixel range sizes are larger and more variable in the near-range due to stronger layover from higher signal-to-noise ratios (SNR) [*Fjørtoft et al.*, 2014]. The higher variability in the mean height bias and area bias above an aspect ratio of twenty is likely the result of this phenomenon. Changing the aspect ratio of the reservoir means it will either capture more or less of the near-range portion of the swath, leading to shifts in the accuracy relative to adjacent aspect ratios.

During the actual mission, it is expected that utilizing results from multiple orbit passes over a single reservoir will help to minimize the area error emanating from dominant coverage in the near-range portion of the swath. This is an iterative process – the greater the number of observations, the better the accuracy. Given this, the error will improve much sooner for reservoirs located at higher altitudes where SWOT repeat passes will be more frequent. However, the shape, size, and orientation of the reservoir will also play a role in the number of repeat observations by different swaths, thereby compounding this problem. For this reason, although potentially achievable using multiple simulations from SWOTsim, we felt it was necessary to instead focus our efforts in determining observation accuracy of reservoirs on cases where the reservoir is largely intersected by a single swath. Analysis of improving reservoir area observations with the use of multiple swaths is too complicated and different of a problem, making it better suited for another study.

According to the topographic results for the theoretical reservoirs, increases in surrounding topography enhanced the bias for both reservoir surface area and height. This phenomenon is largely the result of topographic layover, which is expected to be an issue when the slope of the local terrain exceeds the incidence angle of 0.6–3.9° [*Fjørtoft et al.*, 2014]. Similar to the shape and orientation test results, the bias in height measurements was more variable with changes in slope making it difficult to ascertain the influence of layover. However, the height RMSE was found to be 23% higher for larger slopes above 0.8 m/m, thereby still indicating the presence of stronger layover at higher slopes.

The same phenomenon involved with the irregularities observed in the theoretical reservoir results for shape and orientation was explored further with the experiments involving the effects of partial reservoir coverage. With the exception of the parallel to orbit series of tests, the magnitude in height bias for the

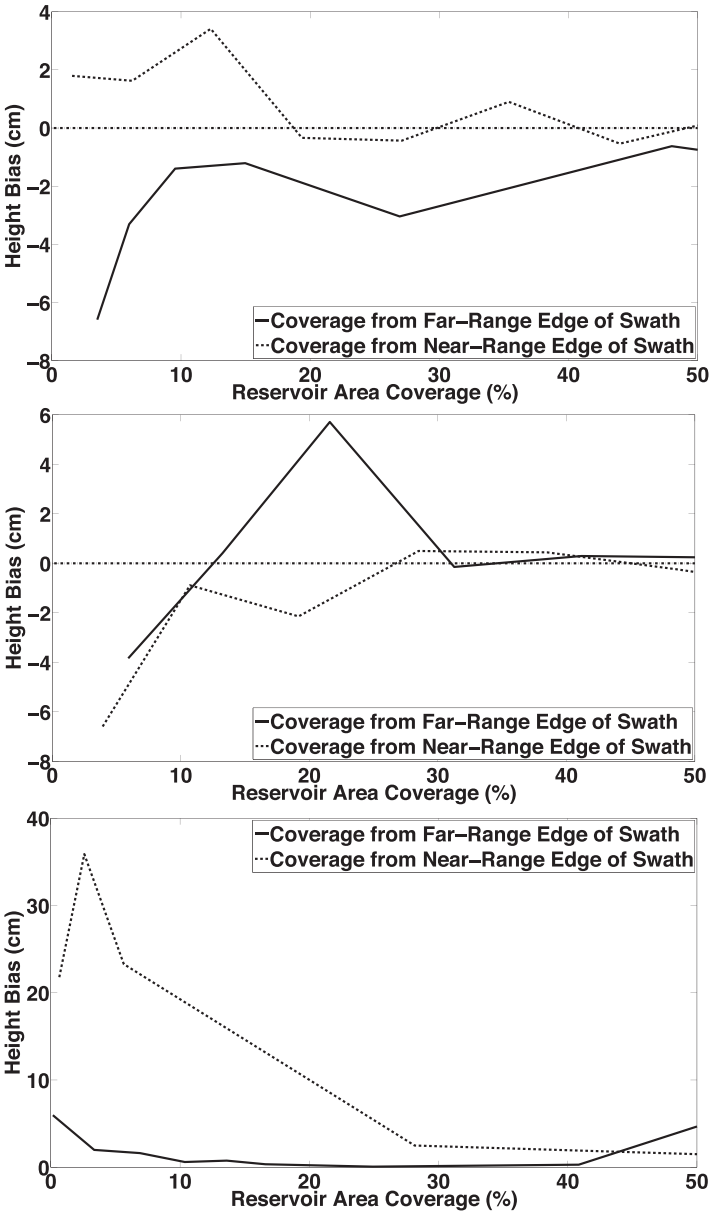

Figure 9. Mean bias in water surface height for partial swath coverage of reservoirs with (top) 1:1 aspect ratio and 24:1 aspect ratios oriented (middle) perpendicular to orbit and (bottom) parallel to orbit, as determined by SWOTsim. Analyses conducted for reservoir sizes of approximately 10^1 km^2.

near and far range experiments was similar given the same percent reservoir area coverage. The larger discrepancies observed in parallel to orbit tests is likely due to higher layover in the near range from larger SNR, as observed in the shape and orientation experiments. The reduction in bias to near-zero for all simulations above 30% reservoir coverage represents an important finding for the reliability of reservoir height estimates that are not completely covered by the swath, as partial swath coverage observations of water bodies are expected to be common occurrences during the actual mission.

4.3. Spatial Analysis: Actual Reservoir Experiments

Results from the SWOTsim simulations involving actual reservoirs in California corroborated the findings from the theoretical reservoir experiments. The smallest reservoir again had the largest median in area bias values. The median height bias results were not as strongly linked to reservoir size, which was due to the higher variability in height accuracies stemming from reservoir shape and orientation or topographic layover effects that were demonstrated in the theoretical experiments. The median height bias values were still within the range of anticipated values shown in the theoretical experiments, as all were less than 15 cm with the exception of the fourth largest reservoir (18.45 km^2). As expected from the reservoir shape and orientation experiments, a much larger range in the 25^{th} to 75^{th} percentile biases and median height bias occurred for the fourth largest reservoir due to its strong parallel-to-orbit orientation. Also as anticipated from previous results, outliers and higher biases for the fourth largest reservoir occurred when swath coverage of the reservoir was predominantly in the near-range, which led to higher layover from increased SNR. In spite of these high biases observed in individual results, the large number of simulations conducted for each reservoir largely cancelled out the effects of the outliers on the median, and the 25^{th} to 75^{th} percentile range for most of the reservoirs.

Testing the influence of reservoir shape on observation accuracy with the true reservoir simulations was avoided because in reality reservoirs come in too many different shapes to adequately quantify this when only six reservoirs were used. The impact of reservoir shapes on observation error was still tested with the

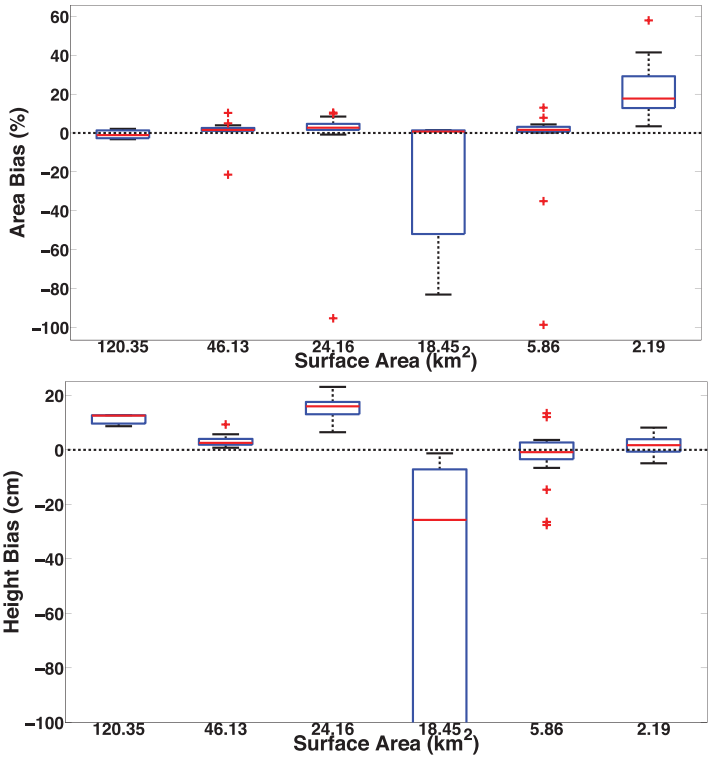

Figure 10. Box plots of (top) area and (bottom) height bias for six California reservoirs. Multiple simulations represented by each plot. Median represented by red line and boxes indicate the 25th and 75th percentiles. Outliers denoted by red crosses and whiskers extend to range of values not considered a statistical outlier. Lower range of 25th to 75th (−900 cm) and whisker (−2300 cm) not shown to focus on distribution of median values relative to 0 cm.

theoretical reservoirs because within this more experimental setting, the expected error range could be captured by testing reservoirs with extreme shapes, such as very high aspect ratios oriented both parallel and perpendicular to orbit. In doing so, the maximum amount of error resulting from the shape of the reservoir was effectively constrained, which was our intent. The number of real reservoirs that could be tested was restricted due to the computational limitations of SWOTsim, so much of the discussion of the true reservoir simulation results focuses on verification of the theoretical reservoir simulation results.

Ideally, SWOTsim would have been run over every reservoir across the globe. However, running SWOTsim over a global DEM (or even California) at the necessary spatial scale is too computationally intensive to generate results in a reasonable amount of time. As such, the theoretical reservoir experiments were devised to represent the expected range of global error stemming from each spatial error source more simply and verified these results with the six California reservoir simulations. In this way, one can still get a general quantitative sense of how much spatial error will occur for any given global reservoir by matching its spatial characteristics to the spatial error properties we find here. We go through this procedure with one of the reservoirs that was tested in Figure 12.

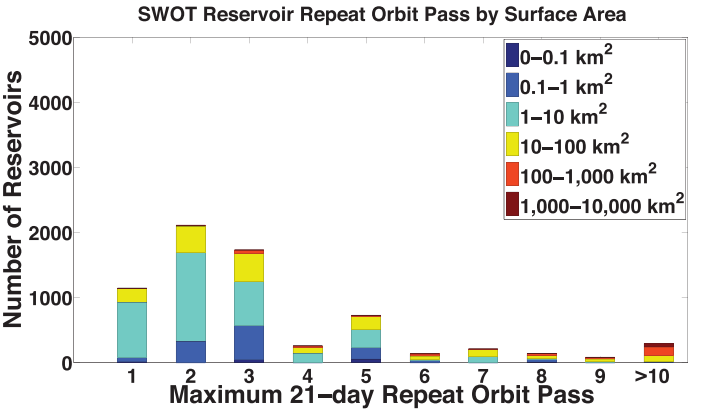

Figure 11. Expected SWOT repeat orbit pass frequencies for global reservoirs colored according to reservoir size: 0–0.1 km^2 (dark blue), 0.1–1 km^2 (blue), 1–10 km^2 (light blue), 10–100 km^2 (yellow), 100–1000 km^2 (orange), 1000–10,000 km^2 (dark red). Estimates derived from the number of repeat orbit passes intersecting a reservoir over a given SWOT cycle, which includes only partial swath coverage based on the expected ability to use ancillary data to reproduce accurate inundated areas and derivation of accurate height measurements demonstrated in this study (Data used to make plots obtained from the Centre National d'Études Spatiales (CNES) and global reservoir data set from *Lehner et al.* [2011].

Results from the analysis in Figure 12 show a total error of 0.88–1.40 km^2, representing 2.35–3.74% of the aggregate total area of the eight ellipses used to make this calculation. The total percent bias is reasonably close to the median error value of 0.72% presented in Figure 10 for the Black Butte Reservoir, thereby verifying that this method can be used to estimate area errors for any global reservoir. Only eight ellipses were used here as a means of

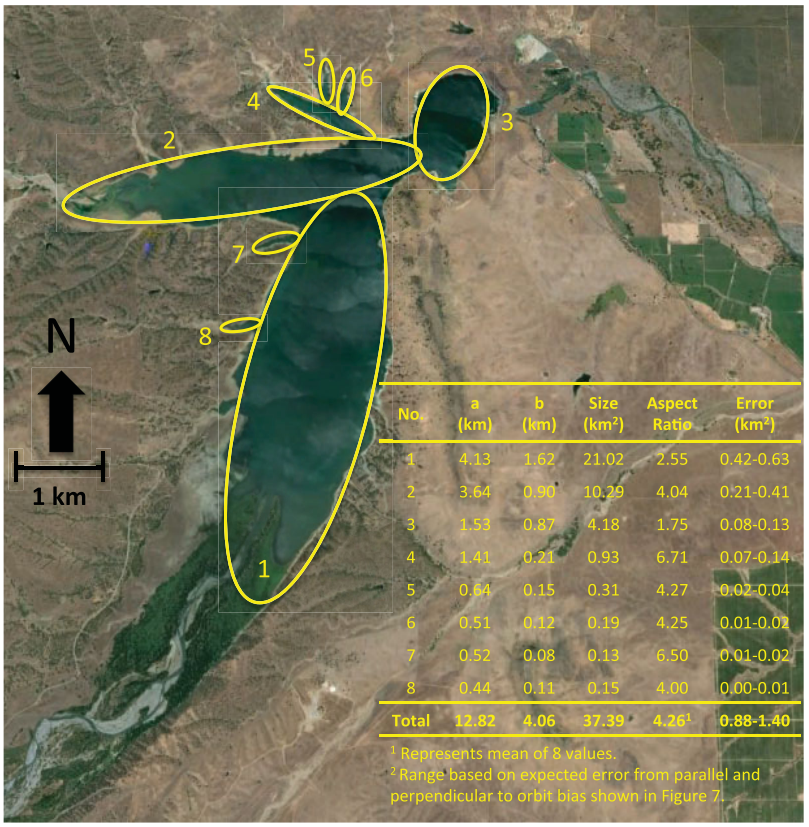

No.	a (km)	b (km)	Size (km^2)	Aspect Ratio	Error (km^2)
1	4.13	1.62	21.02	2.55	0.42-0.63
2	3.64	0.90	10.29	4.04	0.21-0.41
3	1.53	0.87	4.18	1.75	0.08-0.13
4	1.41	0.21	0.93	6.71	0.07-0.14
5	0.64	0.15	0.31	4.27	0.02-0.04
6	0.51	0.12	0.19	4.25	0.01-0.02
7	0.52	0.08	0.13	6.50	0.01-0.02
8	0.44	0.11	0.15	4.00	0.00-0.01
Total	12.82	4.06	37.39	4.26[1]	0.88-1.40

[1] Represents mean of 8 values.
[2] Range based on expected error from parallel and perpendicular to orbit bias shown in Figure 7.

Figure 12. Estimation of area error for Black Butte Reservoir using results from theoretical reservoir experiments presented in Figure 7. Elliptical areas calculated using formula: $a \times b \times \pi$ where a is the major axis and b is the minor axis. Image from *Google Earth* [2013].

demonstrating this method, but we acknowledge disaggregating the reservoir shape into different numbers of ellipses may be used, depending on the desired level of accuracy when applying this technique. Furthermore, we point out that errors due to reservoir topography were not accounted for in this calculation, as topography biases were shown to contribute less than 0.3% for a reservoir of approximately the same size as Black Butte (Figure 8). Although small, we note here that these errors might increase for smaller reservoirs where the error due to topographic interference would represent a greater portion of the total reservoir surface area.

4.4. Study Limitations and Caveats

We chose not to go through a similar procedure to determine height errors for the Black Butte Reservoir due to the much higher variability in height biases from the changes in shape and orientation shown in Figure 7. These errors are potentially further compounded by the large height biases associated with layover from surrounding topography, which would also apply had we taken this additional step. Instead, we point out here that with the exception of reservoirs displaying more extreme spatial configurations and/or those situated adjacent to highly variable topography, the height bias results we present here are largely in agreement with the specifications reported in *Rodriguez* [2015]. As such, when attempting to apply the results from this study to estimate reservoir height biases for SWOT observations, we encourage the use of +/- 10 cm as the maximum water surface height bias for reservoirs above 1 km^2 and +/- 25 cm bias for those between 0.0625 km^2 and 1 km^2 except when the reservoir exists in more extreme geospatial conditions, such as is the case for the fourth smallest actual reservoir that was tested in this study.

SWOTsim was used to evaluate the observation accuracy of exclusively reservoir surface area and elevation. It is noted that other types information will be gathered from observations of these two fields that we did not explore here. For example, reservoir area-elevation relationships can be used to better understand the bathymetry to improve estimates of storage. Furthermore, the product of these two terms can be used to determine changes in storage, which can also be used to estimate storage if the initial volume is known.

However, we chose to focus the evaluation from this study on the accuracy of primary observations of water surface area and elevation that will be made by SWOT, as well as any error resulting from the expected frequency of observations. Although important, exploration of how well SWOT will be able to reproduce area-elevation relationships and storage changes is outside the scope of the work in this study.

It is further acknowledged that the six reservoirs used in the actual reservoir test cases fall short of the total number of reservoirs found worldwide. Using a small subset of reservoirs for this study component was conducted for two reasons. First, running the simulator for every reservoir was impractical due to the intense computation time required to complete such an endeavor. Second, SWOTsim is constantly being updated and improved. Later SWOTsim releases are expected to be more representative of actual SWOT measurements and may facilitate application over much larger areas as alogrithms used to process the data evolve and computation times decrease. Newer versions of the simulator are expected to have additional modules to improve the water surface location and land classification errors relative to the version that was used in this study. Furthermore, as SWOTsim is only a model, results should be considered as mere representations of reality based on the current state-of-the-art physical understanding of what the satellite will observe. True accuracy in observations will only be realized during the actual mission. The results shown in this study, although improving upon the understanding of expected error characteristics of reservoirs from SWOT, should thus be used as a benchmark to guide future work with SWOT reservoir observations rather than accepted as the absolute truth.

It is also important to note that the largest surface area of the six reservoirs that were tested was less than 120 km^2 even though the largest reservoir surface area found worldwide exceeds 66,000 km^2 [*Lehner et al.*, 2011]. Excluding this size class from the study was justified, however, because the bias in reservoir surface area diminished to less than 1% of the total surface area and mean bias in height was representative of others in both the reservoir test cases and theoretical experiments. Moreover, as demonstrated in the theoretical experiments, the area and height biases were smallest for the largest theoretical reservoir that was tested of 10,000 km^2, which is much closer to the high end of the range of global surface areas. Thus, omitting the larger size classes from the analysis was not believed to result in the loss of much additional information.

5. Conclusions

This study characterized the temporal and spatial errors of SWOT reservoir observations using a combination of in situ reservoir records and model results. It represents the first study known to the authors to investigate the SWOT observation accuracy exclusively for man-made reservoirs and not just natural lakes. In addition, this was accomplished using SWOTsim, which integrates error properties of the instrument and satellite orbit, thereby making the results more comparable to what is expected from the actual mission than what has previously been accomplished for lakes or reservoirs at this level of spatial and temporal resolution.

Despite the previously noted limitations, several important temporal and spatial performance thresholds were highlighted throughout the course of the study. The temporal analysis showed that converting SWOT observations to monthly values does not result in severe aliasing except for with the smaller reservoir sizes (<3 km^2) at the lowest expected satellite orbit return interval where errors of up to 10% were observed for a single observation. Based on the cumulative distribution function (CDF) for reservoir surface areas shown in Figure 2, less than 13% of reservoirs worldwide considered to be observable by SWOT are expected to fall under this size class as well as sampled at low enough frequencies to where temporal aliasing might pose an issue.

The theoretical and test case reservoir simulations revealed that reservoir size has the largest influence on the accuracy of SWOT surface area and height measurements. Reservoirs larger than 1 km^2, which account for approximately 80% of those observed globally, are expected to have surface area and height biases of less than 5% and -5 cm, respectively. Errors for reservoir sizes below the 1 km^2 threshold increased exponentially up to an area bias of 21% and height bias of -20 cm. In certain situations, specific geospatial characteristics of the reservoir played a larger role in SWOT water surface area and height observation errors. For instance, higher elliptical aspect ratios and orientation of the reservoir parallel to orbit were observed to increase errors by up to factors of three and six for surface area and height estimates, respectively, in the

three more common reservoir sizes that were tested. Increases in surface area errors due to rises in topographic slope were most dramatic around a slope of 0.17 m/m and the height RMSE was 23% higher for slopes above 0.8 m/m relative to slopes below this magnitude. The partial reservoir coverage tests revealed that above 30% coverage of the reservoir for all spatial configurations and orientations, height estimates were reliable and showed a near-zero bias. Swath coverage that was dominated in the near range also resulted in much higher error estimates for both area and height measurements. Evidence from the actual reservoir simulations agrees with these findings, as larger reservoirs (>2 km^2) result in smaller area and height biases, except in the instance where the reservoir had a more extreme elliptical geometry oriented parallel to orbit or swath coverage is concentrated in the near-range.

The findings presented herein provide more in-depth insight into future SWOT reservoir observations. As the development of SWOTsim improves, additional simulations of reservoirs and other surface water features will only continue to be more representative of expected SWOT global surface water observations. Even still, the results presented here represent the first, more realistic attempt at reproducing global reservoir behavior as seen by SWOT. This information will be useful for determining SWOT error characteristics of a given specific reservoir a priori to mission launch and should serve as a blueprint for subsequent studies that incorporate SWOT reservoir observations into global monitoring systems or hydrologic models.

Appendix A

Appendix A1 lists the user-specified SWOTsim instrument simulator settings that were used for all analyses requiring SWOTsim (e.g. Figures 6–9 and Tables 1 and 2). The settings and parameters listed are related to the satellite resolution geometry, radar parameters, and beam. parameters.

Table A1. SWOTsim Instrument Simulator Settings and Parameters

Setting or Parameter	Value
Resolution Geometry	
Azimuth spacing (m)	30
Swath width (m)	140000
Ground spacing (m)	30
Number of landtypes	2 (water and land)
Near range (m)	895810
Number of interferogram pixels	3,860
Radar Parameters	
Peak transmit power (W)	1,500
Receive noise figure (dB)	8
System loss (dB)	4.5
Point target response range length (m)	3
Operational mode	NPP
Beam Parameters	
Wavelength (m)	0.0084
Pulse repetition frequency (PRF) (Hz)	4420
Pulse duration (us)	4.5
Signal bandwidth (MHz)	200
Sampling frequency (MHz)	200
Velocity (m/s)	7415.3
Ground velocity (m/s)	6506.4
Percent processing pulse repetition frequency (PRF) bandwidth (%)	100
Integrated sidlobe ratio (ISLR) (dB)	13.0
Baseline (m)	10.0
Polarization	Horizontal
System noise temperature (K)	3681.79

Acknowledgments
The SWOTsim instrument simulator (v2, acquired 1 October 2014) provided much of the data that were used in this study and is under ongoing development. A portion of this work was conducted at the Jet Propulsion Laboratory, California Institute of Technology (JPL-Cal Tech), under contract with NASA. In situ data were obtained from the California Department of Water Resources California Data Exchange Center (www.cdec.water.ca.gov, accessed 18 August 2014). Digital Elevation Model (DEM) data used in this study came from the NASA ASTER GDEM v2 at 30 m resolution (http://gdex.cr.usgs.gov/gdex/, accessed 5 December 2014). The authors are particularly grateful for the generous financial support received from the National Aeronautics and Space Administration (NASA) Earth and Space Science Fellowship (NESSF) for this research. We would also like to thank members of the SWOT Science Definition Team, in particular Konstantios M. Andreadis and Brent A. Williams for providing assistance and information on the SWOTsim instrument simulator. The authors John T. Reager and James S. Famiglietti were partially supported by the Jet Propulsion Laboratory, California Institute of Technology, under a contract with NASA.

References

Alsdorf, D. E., E. Rodriguez, and D. P. Lettenmaier (2007), Measuring surface water from space, *Rev. Geophys.*, *45*, RG2002, doi:10.1029/2006RG000197.

Andreadis, K. M., E. A. Clark, D. P. Lettenmaier, and D. E. Alsdorf (2007), Prospects for river discharge and depth estimation through assimilation of swath-altimetry into a raster-based hydrodynamics model, *Geophys. Res. Lett.*, *34*, L10403, doi:10.1029/2007GL02721.

Baros, N., J. J. Cole, L. J. Tranvik, Y. T. Prairie, D. Bastviken, V. L. M. Huszar, P. del Giorgio, and F. Roland (2011), Carbon emission from hydroelectric reservoirs linked to reservoir age and latitude, *Nature Geosci.*, *4*, 593–596.

Biancamaria, S., K. M. Andreadis, M. Durand, E. A. Clark, E. Rodriguez, N. M. Mognard, D. E. Alsdorf, D. P. Lettenmaier, and Y. Oudin (2010), Preliminary characterization of SWOT hydrology error budget and global capabilities, *J. Selec. Top. Appl. Earth Obs. Remote Sens.*, *3*, 6–19, doi:10.1109/JSTARS.2009.2034614.

Biancamaria, S., D. P. Lettenmaier, and T. M. Pavelsky (2015), The SWOT mission and its capabilities for land hydrology, *Surv. Geophys.*, doi: 10.1007/s10712-015-9346-y. [Available at http://ascelibrary.org/doi/ref/10.1061/%28ASCE%29HE.1943-5584.0001320.]

Chao, B. F., Y. H. Wu, and Y. S. Li (2008), Impact of artificial reservoir water impoundment on global sea level, *Science*, *320*, 212–214, doi: 10.1126/science.1154580.

Cooke, G. D., E. B. Welch, S. A. Peterson, and S. A. Nichols (2005), *Restoration and Management of Lakes and Reservoirs*, 3rd ed., 601 pp., Taylor and Francis, Boca Raton, Fla.

Crétaux, J.F., S. Biancamaria, A. Adalbert, M. Bergé-Hguyen, and B. Mélanie (2015), Global surveys of reservoirs and lakes from satellites and regional application to the Syrdarya river basin, *Environ. Res. Lett.*, *10*, 1–13, doi:10.1088/1748-9326/10/1/015002.

Durand, M., K. M. Andreadis, D. E. Alsdorf, D. P. Lettenmaier, D. Moller, and M. Wilson (2008), Estimation of bathymetric depth and slope from data assimilation of swath altimetry into a hydrodynamic model, *Geophys. Res. Lett.*, *35*, L20401, doi:10.1029/2008GL034150.

Durand, M., E. Rodriguez, D. E. Alsdorf, and M. Trig (2010), Estimating river depth from remote sensing interferometry measurements of river height, slope, and width, *IEEE J. Selec. Top. Appl. Earth Obs. Remote Sens.*, *3*, 20–31, doi:10.1109/JSTARS.2009.

Eilander, D., F. O. Annor, L. Iannini, and N. van de Giesen (2014), Remotely sensed monitoring of small reservoir dynamics: A Bayesian approach, *Remote Sens.*, *6*, 1191–1210, doi:10.3390/rs6021191.

Famiglietti, J. S., A. Cazenave, A. Eickler, J. T. Reager, M. Rodell, and I. Velicogna (2015), Satellites provide the 'big picture,' *Science*, *14*, 684–685, doi:10.1126/science.aac9238.

Fjørtoft, R., et al. (2014), KaRIn on SWOT: Characteristics of Near-Nadir Ka-Band Interferometric SAR Imagery, *IEEE Trans. Geosci. Remote Sens.*, *52*, 2172–2185, doi:10.1109/TGRS.2013.2258402.

Gao, H., C. Birkett, and D. P. Lettenmaier (2012), Global monitoring of large reservoir storage from satellite remote sensing, *Water Resour. Res.*, *48*, W09504, doi:10.1029/2012WR012063.

Google Earth (2013), *V. 7.1.5.1557, 39°46'55.48"N 122° 20'44.42"W, eye alt 42,122 ft*, DigitalGlobe 2015. [Available at http://www.earth.google.com, last accessed 17 Nov. 2015].

Hanasaki, N., S. Kanae, and T. Oki (2006), A reservoir operation scheme for global river routing models. *J. Hydrol.*, *327*, 22–41, doi:10.1016/j.hydrol.2005.11.011.

Lee, H., M. Durand, H. C. Jung, D. E. Alsdorf, C. K. Shum, and Y. Sheng (2010), Characterization of surface water storage changes in Arctic lakes using simulated SWOT measurements, *Int. J. Remote Sens.*, *31*, 3931–3953, doi:10.1080/01431161.2010.483494.

Lehner, B., et al. (2011), High-resolution mapping of the world's reservoirs and dams for sustainable river-flow management, *Frontiers Ecol. Environ.*, *9*, 494–502, doi:10.10890/100125.

Moller, D., K. Andreadis, E. Rodriguez, X. Wu, and D. Alsdorf (2010), A virtual mission to estimate discharge using assimilation of high-resolution simulated SWOT data: Initial results over the Ohio River, *Proc. SPIE*, *782617-1–782617-10*, doi:10.11117/12.868979.

Munier, S., A. Polebistki, C. Brown, G. Belaud, and D. P. Lettenmaier (2015), SWOT data assimilation for operational reservoir management on the upper Niger River Basin, *Water Resour. Res.*, *51*, 554–575, doi:10.1002/2014WR016157.

NOAA (2014), National Climatic Data Center, State of the Climate: Drought for March 2014. [Available at http://www.ncdc.noaa.gov/sotc/drought/2014/3, last accessed 8 Sep. 2014.]

Pavelsky, T. M., M. T. Durand, K. M. Andreadis, R. E. Beighley, R. C. D. Paiva, G. H. Allen, and Z. F. Miller (2014), Assessing the potential global extent of SWOT river discharge observations, *J. Hydrol.*, *519*, 1516–1525, doi:10.1016/j.hydrol.2014.08.044.

Peral, E., E. Rodriguez, D. Moller, M. McAdams, M. Johnson, K. Andreadis, D. Arumugam (2012), *SWOT L1b Hydrology Simulator User Guide, Version 2.1*, Jet Propul. Lab., Pasadena, Calif.

Rodriguez, E. (2015), SWOT Science Requirements Document, *JPL Doc. D-61923*. [Available at http://swot.jpl.nasa.gov/files/SWOT_science_reqs_final.pdf, last accessed 6 Feb. 2016.]

Rodriguez, E., and D. Moller (2004), Measuring surface water from space, *Eos Trans. AGU*, *85*(47), Fall Meet. Suppl., Abstract H22C-08.

Schneider, P., and S. J. Hook (2010), Space observations of inland water bodies show rapid surface warming since 1985, *Geophys. Res. Lett.*, *37*, L22405, doi:10.1029/2010GL045059.

Smith, L., and T. Pavelsky (2009), Remote sensing of volumetric storage changes in lakes, *Earth Surf. Processes Landforms*, *34*, 1353–1358, doi:10.1002/esp.1822

Syed, T. H., J. S. Famiglietti, D. P. Chambers, J. K. Willis, and K. Hilburn (2010), Satellite-based global-ocean mass balance estimates of interannual variability and emerging trends in continental freshwater discharge, *Proc. Natl. Acad. Sci. U. S. A.*, *42*, 17,916–17,921, doi:10.1073/pnas.1003292107.

Williamson, C.E., J. E. Saros, and D. W. Schindlerm (2009), Sentinels of change, *Science*, *323*, 887–888, doi:10.1126/science.1169443.

World Commission on Dams (2000), *Dams and Development: A Framework for Decision Making*, Earthscan Publ., London, U. K.

Yoon, Y., and E. Beighley (2014), Simulating streamflow on regulated rivers using characteristic reservoir storage patterns derived from synthetic remote sensing data, *Hydrol. Processes*, *29*, 2014–2026, doi:10.1002/hyp.10342.

Zhang, J., K. Xu, Y. Yang, L. Qi, S. Hayashi, and M. Watanabe (2006), Measuring water storage fluctuations in Lake Dongting, China, by TOPEX/POSEIDON satellite altimetry, *Environ. Monit. Assess.*, *115*, 23–37, doi:10.1007/s10661-006-5233-9.